Nitrile Rubber/Organomontmorillonite Nanocomposites Produced by Solution and Melt Compounding: Effect of the Polarity of the Quaternary Ammonium Intercalants

Bluma G. Soares,[1] Marlucy de Oliveira,[1] Soraia Zaioncz,[1] Ana C. O. Gomes,[1] Adriana A. Silva,[1] Kelly S. Santos,[2] Raquel S. Mauler[2]

[1]*Instituto de Macromoléculas, Universidade Federal do Rio de Janeiro, Centro de Tecnologia, Bloco J, Ilha do Fundão, Rio de Janeiro, RJ, Brazil 21945-970*
[2]*Instituto de Química, Universidade Federal do Rio Grande do Sul, Avenida Bento Gonçalves 9500, Porto Alegre, RS, Brazil 91501-970*

Received 20 November 2009; accepted 15 April 2010
DOI 10.1002/app.32649
Published online 27 July 2010 in Wiley Online Library (wileyonlinelibrary.com).

ABSTRACT: A comparative study of the development of nitrile rubber (NBR) based nanocomposites was performed; two organomontmorillonites (Cloisite 15A and Cloisite 30B) and two procedures for clay dispersion (melt blending and solution intercalation) were used. The nanocomposites were cured with a system based on dicumyl peroxide in the presence of *m*-phenylenebismaleimide as a coagent for curing. The dispersion of the organoclay inside the NBR matrix was investigated with transmission electron microscopy and X-ray diffraction. All the cured systems displayed a combination of intercalated, partially exfoliated clay platelets and confined, deintercalated clay; the degree of dispersion depended on the amount of clay, the type of intercalant, and the intercalation procedure. The highest amount of intercalated/exfoliated clay was obtained with a previous dispersion of the clay (Cloisite 30B) in an NBR solution. All the nanocomposites presented outstanding tensile strength and creep response, and this indicated a reinforcing effect of the layered silicates. © 2010 Wiley Periodicals, Inc. J Appl Polym Sci 119: 505–514, 2011

Key words: clay; creep; elastomers; nanocomposites; X-ray

INTRODUCTION

Nitrile rubber (NBR) nanocomposites based on layered silicates have attracted great interest because they are able to provide improved mechanical and thermal properties in comparison with those containing conventional fillers (e.g., carbon black and precipitated silica) at similar concentrations. The outstanding properties of these so-called nanocomposites are based on the extremely large contact surface and high aspect ratio achieved with the intercalation/exfoliation process and on the homogeneous dispersion of individual silicate platelets in the polymer matrix.[1] Montmorillonite (MMT) clay is the most commonly used layered silicate because of its natural occurrence and the feasibility of exchanging the interlayer inorganic cations for organic cations, such as ammonium cations with long aliphatic hydrocarbon chains. This modification ensures better compatibilization of the clay with the polymer matrix.[2–4] The development of NBR-based nanocomposites with layered silicates is relatively new and involves different procedures, such as the cocoagulation of NBR latex with an aqueous clay dispersion,[5,6] the dispersion of clay in a solution containing NBR,[7–9] and melt intercalation.[10–22]

The method used for clay dispersion, the composition of NBR, the nature of the organic ammonium cation used in the functionalization of the clay, and the curing process affect the degree of exfoliation and also the physicomechanical properties of the corresponding nanocomposites. Sadhu and Bhowmick[8] dispersed pristine clay or organoclay into NBR with the solution procedure. They observed a slight increase in the clay gallery gap when pristine clay was employed. However, with the organoclay, intercalation or exfoliation was observed only with NBR containing lower amounts of acrylonitrile, that is, less polar NBR samples. Using a two-roll mill, Choi et al.[11] dispersed an organoclay in an NBR matrix with 33% acrylonitrile, and they observed a shift in the X-ray diffraction (XRD) peak (related to the basal spacing of the organoclay) toward higher 2θ values after curing (θ is the angle of incident radiation); this indicated a reduction of the *d*-spacing (*d* is the interplanar distance). They suggested a deintercalation process and the formation of some aggregates. By adding a complex composed of resorcinol

Correspondence to: B. G. Soares (bluma@ima.ufrj.br).
Contract grant sponsors: Conselho Nacional de Desenvolvimento Científico e Tecnológico, Coordenação de Aperfeiçoamento de Pessoal de Nível Superior, Fundação de Amparo à Pesquisa do Estado do Rio de Janeiro.

and hexamethylenetetramine, Liu et al.[16] observed some degree of exfoliation in melt-processed nanocomposites composed of NBR (with 29% acrylonitrile) and organoclay. In a series of interesting articles, Kim and coworkers[12–14] observed a high degree of exfoliation when an organoclay was processed with NBR (with 29% acrylonitrile) in the melt. Han et al.[23] used organically modified MMT containing vinyl groups. This system was cured with a sulfur system and presented a nanocomposite structure that was both exfoliated and intercalated. Das et al.[24,25] studied the influence of peroxide and sulfur systems as curing agents for NBR/clay and carboxylated NBR/clay nanocomposites[26] and found a higher ordered orientation of the clay platelets in peroxide-cured matrices.

In this article, we evaluate the intercalation/exfoliation degree of two different MMT-based organoclays, Cloisite 15A (OC15A) and Cloisite 30B (OC30B), dispersed into an NBR matrix and the mechanical and dynamic mechanical properties (especially the creep response) of the corresponding nanocomposites. The choice of these organoclays was based on the differences in the polarity of the intercalants, which should influence the interaction between the organoclay and the polar rubber: the first, OC15A, contains a less polar intercalant based on dimethyl ditallow quaternary ammonium salt, and the second, OC30B, is more polar and contains methyl tallow bis(2-hydroxyethyl)quaternary ammonium as the intercalant.

A peroxide-based curing system in combination with *m*-phenylenebismaleimide (BMI) as the coagent was employed for curing. Peroxide-based systems present several advantages because they require simpler formulations without too many ingredients and the byproducts generated during the curing process are less toxic than those generated by sulfur systems. In addition, the corresponding vulcanizates usually present relatively high temperature resistance, good elastic behavior (especially compression set), higher aging resistance, and no discoloration of the finished products.[27] The use of bismaleimide is also interesting because it can improve the curing efficiency, take part in the network through its double bonds, and give rise to crosslinks very stable against heat.[28]

EXPERIMENTAL

Materials

NBR {acrylonitrile content = 45%; Mooney viscosity [ML(1+4) at 100°C] = 60} was kindly supplied by Petroflex (Rio de Janeiro, Brazil). The organoclays used in this study were supplied by Southern Clay Products (Louisville, KY): OC30B [a natural MMT modified with methyl tallow bis(2-hydroxyethyl)-quaternary ammonium with a cationic-exchange capacity of 90 mequiv/100 g] and OC15A (a natural MMT modified with dimethyl ditallow quaternary ammonium salt with a cationic-exchange capacity of 125 mequiv/100 g). BMI was purchased from DuPont Dow Elastomers (Freeport, TX) with the trade name HVA-2. Dicumyl peroxide (DCP) was supplied by Retilox (São Paulo, Brazil).

Preparation of the nanocomposites

Melt intercalation

NBR/organoclay nanocomposites were prepared in a Brabender (Duisburg, Germany) plastograph equipped with a W50 EHT internal mixer with Banbury blades and operated at a rotor speed of 80 rpm with a fill factor of 0.85. NBR was first masticated at 80°C for 2 min and then mixed with the organoclay for 13 min. During the blending, the mixing temperature was increased to approximately 130°C. The compounded rubber was then transferred to an open two-roll mill, and the curatives (1 g of DCP and 1 g of BMI with respect to 100 g of rubber) were added.

Solution intercalation

A master batch with an NBR/clay weight ratio of 2 : 1 was first prepared by the dispersion of 10 g of clay in 140 mL of a solvent (chloroform for OC15A and tetrahydrofuran for OC30B) via mechanical stirring at 50°C for 4 h. Then, a solution composed of 20 g of NBR in 200 mL of chloroform or tetrahydrofuran was slowly added, and the resulting dispersion was sonicated in a Branson sonicator (Danbury, Connecticut) with a 10-kV amplitude for 15 min. After this treatment, the dispersion was precipitated into methanol and dried *in vacuo*. An appropriate amount of this master batch was compounded with NBR in a two-roll mill to achieve the desired proportion of clay, and this was followed by the curatives (BMI/DCP = 1 g/1 g with respect to 100 g of rubber).

The samples were compression-molded in a hydraulic press at 170°C at a pressure of 5 MPa. The molding time was adjusted according to the optimum cure time (ASTM method D 2084-81), which was determined with an oscillating disk rheometer (model T100, Tecnologia Industrial, Buenos Aires, Argentina) with an oscillating angle of 1°. The optimum cure time was established as the time to reach 90% of the maximum torque (t_{90}). The test specimens (2.0 mm thick) for tensile analysis and dynamic mechanical analysis (DMA) were cut from the molded slabs. The test specimens for XRD measurements were prepared from approximately 0.5-mm molded slabs.

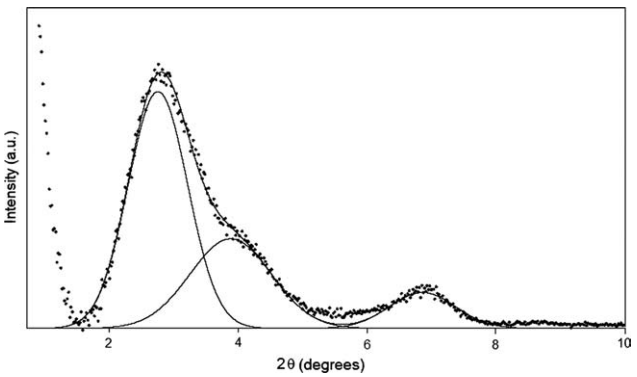

Figure 1 XRD pattern of Cloisite 20A with the corresponding deconvoluted peaks.

Characterization and testing

XRD studies were performed on a Rigaku (Tokyo, Japan) Ultima IV X-ray diffractometer (40 kV and 20 mA) in the 2θ range of 0.5–10°. The *d*-spacing of the clay particles was calculated with the Bragg equation:

$$n\lambda = 2d \sin \theta \tag{1}$$

where n is an integer determined by the order given and λ is the wavelength of the X-ray (for the copper target used here, λ was 1.54 Å). The XRD peaks were submitted to a deconvolution treatment with free peak-fitting software called *fityk*. [*fityk* is a program for nonlinear fitting of analytical functions (especially peak-shaped) to data (usually experimental); it can be downloaded at http://www.unipress.waw.pl/fityk.] Figure 1 illustrates this methodology with the XRD results for the commercial organoclay Cloisite 20A. The percentage of the intercalated clay with different *d*-spacings was calculated by the relation of the area of the corresponding diffracted peak obtained by the deconvolution process to the total area of the diffracted peaks.

Transmission electron microscopy (TEM) was performed on a JEOL (Tokyo, Japan) JEM-120 ExII operated at 80 kV. The samples for TEM were cryogenically ultramicrotomed at −80°C in sections approximately 70 nm thick with an RMC Power Tome X microtome (Tucson, Arisona) equipped with a diamond knife at −80°C, and the films were collected onto 300-mesh copper grids.

For tensile testing of the samples, dumbbell-shaped test specimens were used according to DIN method 53504 type S2. The measurements were performed in a universal testing machine (model 5569, Instron, Boston, MA) at a crosshead speed of 200 mm/min at 25°C.

For oil-uptake measurements, the test specimens were immersed in a mineral oil at 100°C for 22 h. The test specimens were then removed from the oil, wiped with tissue paper for removal of the excess oil from the surface, and weighed. The mass swelling (%) was then calculated as follows:

$$\text{Change in mass} = \frac{W_2 - W_1}{W_1} \times 100 \tag{2}$$

where W_1 and W_2 are the weights of the samples before and after immersion, respectively.

A DMA Q-800 dynamic mechanical analyzer from TA Instruments (New Castle, DE) was used for determining the modulus and glass-transition temperature (T_g) and the tensile creep response with single-cantilever and tension modes, respectively. For conventional DMA in the single-cantilever mode, the experiments were performed at a constant frequency of 10 Hz, at a strain amplitude of 30 μm, and at temperatures ranging from −60 to +60°C with a heating rate of 2°C/min. The sample specimen dimensions were 25 × 12 × 2 mm^3. The temperature corresponding to the maximum peak in a tan δ versus temperature plot was taken to be T_g.

Short-time creep tests were carried out with the methodology described by Siengchin and coworkers[29,30] in a DMA Q-800 apparatus (TA Instruments) with the tensile mode at 25°C. The creep and recoverable compliance were determined as a function of time (creep time = 10 min and recovery time = 30 min). A tensile stress of 0.1 MPa was applied. For these experiments, the specimen dimensions were 3 × 1 × 0.5 mm^3 (width × length × thickness).

RESULTS AND DISCUSSION

XRD studies

Figure 2 shows the XRD patterns of the NBR/OC15A clay nanocomposites as a function of the

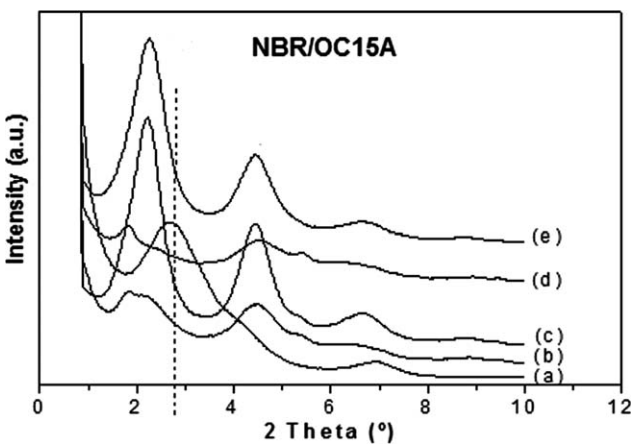

Figure 2 XRD patterns of the NBR/OC15A clay nanocomposites as a function of the amount of clay and the dispersion procedure: (a) pure OC15A, (b) 2.5% clay (melt intercalation), (c) 5.0% clay (melt intercalation), (d) 2.5% clay (solution intercalation), and (e) 5.0% clay (solution intercalation).

TABLE I
XRD Data for NBR/OC15A Nanocomposites as a Function of the Dispersion Procedure and the Amount of Clay

Clay (%)	Dispersion procedure	2θ	*d*-Spacing (nm)	Peak area[a]	Total area	Clay population with specific *d*-spacing (%)	Proportion of intercalated clay (%)[b]	Full width at half-maximum
100 (curve a)	—	2.7	3.3	1700	2526	67	—	1.1
		4.0	2.0	525		21		1.2
		6.8	1.3	315		12		1.2
2.5 (curve b)	Melt	2.1	4.2	730	1676	43	43	1.1
		4.5	2.0	610		36		0.9
		5.4	1.6	52		4		0.4
		6.6	1.3	157		10		1.2
		8.9	1.0	127		7		1.5
5.0 (curve c)	Melt	2.2	4.0	3290	4364	56	56	0.7
		4.4	2.0	1184		29		0.7
		5.3	1.7	49		3		0.4
		6.7	1.3	274		9		0.8
		8.8	1.0	253		3		1.4
2.5 (curve d)	Solution	2.2	4.0	210	1450	15	15	1.1
		4.5	2.0	685		47		1.3
		5.4	1.6	40		3		0.3
		6.3	1.4	405		28		1.7
		8.8	1.0	110		7		1.7
5.0 (curve e)	Solution	2.2	4.0	2160	3997	54	54	0.8
		4.5	2.0	1097		27		0.9
		6.5	1.3	595		15		1.8
		8.7	1.0	145		4		1.6

The curves are illustrated in Figure 1.
[a] The peak area was calculated from the deconvolution of the WAXS peaks.
[b] The intercalated clay was clay with an interlayer *d*-spacing greater than 3.3 nm.

clay concentration and dispersion procedure. Pure OC15A presented its main diffraction peak at $2\theta = 2.7^\circ$, which corresponded to an interlayer spacing of 3.3 nm. Two other small peaks, which appeared at 2θ values of 4.0 and 6.8° (see Fig. 1), could be attributed to some amount of the organoclay with a lower amount of the intercalant in the clay platelets and some pristine clay used for the preparation of OC15A, respectively.[31]

The presence of diffraction peaks for all the NBR/OC15A clay nanocomposites indicated that the clay platelets were not completely exfoliated. However, it was possible to observe different clay populations: one group was related to the XRD pattern appearing at 2θ values lower (larger interlayer spacing) than those found for the original organoclay; this characterized the intercalated dispersion state of the clay. The other clay population with smaller interlayer spacing (higher 2θ values) than that of the original organoclay was also present; this suggested that some amount of the original intercalant was removed from the clay galleries, and this resulted in the collapse of the intercalated structure. This phenomenon was observed in both melt- and solution-intercalated nanocomposites, and this suggested that the deintercalation process was favored during the curing step, as also reported by other authors.[32–34] As the amount of clay increased [Fig. 2(c) for the melt process and Fig. 2(e) for the solution process], the peaks became more intense and narrower; this was suggested by the values of the width at the half-height peak, which indicated an increase in the coherent order of the silicate layers. The proportion of the clay population with a different intercalation degree was determined from the relative area of the peaks obtained after the deconvolution according to the procedure described in the Experimental section. The results are summarized in Table I, which shows that the amount of intercalated clay (*d*-spacing > 3.3 nm) was higher in the melt-intercalated nanocomposites when a lower amount of clay (2.5%) was employed. These phenomena may be attributed to the shear forces imparted to the material during the melt-intercalation process, which favored the penetration of the polymer chain inside the galleries. Increasing the amount of clay resulted in an increase in the proportion of intercalated clay. However, at this higher clay content (5%), the method used for the clay dispersion did not affect this proportion. The values of the width at half-height peaks for the nanocomposites prepared with the previous clay dispersion in the NBR solution were somewhat larger, and this indicated a small decrease in the coherent order of the silicate layers.

The XRD profiles of the NBR-based nanocomposites prepared with OC30B clay are compared to

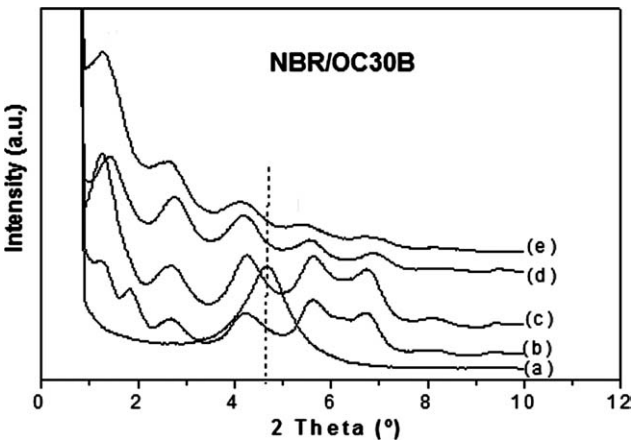

Figure 3 XRD patterns of the NBR/OC30B clay nanocomposites as a function of the amount of clay and the dispersion procedure: (a) pure OC30A, (b) 2.5% clay (melt intercalation), (c) 5.0% clay (melt intercalation), (d) 2.5% clay (solution intercalation), and (e) 5.0% clay (solution intercalation).

that of pure OC30B in Figure 3, and the quantitative analysis of the corresponding peaks is summarized in Table II.

The nanocomposites presented several peaks in the 2θ range of 0.5–10°, which indicated the presence of clay tactoids with different degrees of intercalation together with some deintercalated clay. Also in these composites, there was a great amount of clay in the intercalated form; this was characterized by XRD peaks at 2θ values lower than that corresponding to the original peak of the organoclay, which appeared at $2\theta = 4.7°$ (d-spacing = 1.9 nm). In addition, some amount of the intercalated clay in all NBR/OC30B composites presented basal interlayer distances as high as 6.8 and 7.4 nm, and this clay may be considered almost exfoliated. The amount of intercalated clay was higher for nanocomposites prepared by the solution-intercalation method, with fractions corresponding to approximately 80%, regardless of the amount of clay. These results indicate that NBR chains could penetrate the OC30B galleries to a greater extent, probably because of the presence of polar hydroxyl end groups in the intercalant moieties of this organoclay, which should promote better interactions with polar polymers such as NBR. This phenomenon is more important in solution intercalation.

TABLE II
XRD Data for NBR/OC30B Nanocomposites as a Function of the Dispersion Procedure and Amount of Clay

Clay (%)	Dispersion procedure	2θ	d-Spacing (nm)	Peak area[a]	Total area	Clay population (%)	Proportion of intercalated clay (%)[b]	Full width at half-maximum
100 (curve a)	—	4.7	1.9	1435	1435		—	1.1
2.5 (curve b)	Melt	1.3	6.8	165	2257	7	47	0.5
		1.8	4.9	145		6		0.3
		2.7	3.3	250		12		0.7
		4.3	2.1	495		22		1.0
		5.7	1.5	615		27		0.8
		6.2	1.4	82		4		0.3
		6.7	1.3	420		19		0.7
		8.0	1.1	85		3		1.0
5.0 (curve c)	Melt	1.2	7.3	925	3602	26	55	0.6
		2.7	3.3	270		8		0.7
		4.2	2.1	765		21		0.8
		5.7	1.5	910		25		0.9
		6.3	1.4	67		2		0.3
		6.7	1.3	580		15		0.7
		8.1	1.1	85		3		1.0
2.5 (curve d)	Solution	1.4	6.3	605	1508	40	82	0.5
		2.7	3.3	336		22		0.6
		4.2	2.1	302		20		0.6
		5.6	1.6	112		8		0.5
		6.9	1.3	105		7		0.5
		8.2	1.1	48		3		1.4
5.0 (curve e)	Solution	1.3	6.8	511	1498	34	81	0.5
		2.6	3.4	440		29		0.7
		4.2	2.1	278		18		0.7
		5.4	1.6	132		9		0.8
		6.8	1.3	95		7		0.8
		8.2	1.1	42		3		1.4

The curves are illustrated in Figure 2.
[a] The peak area was calculated from the deconvolution of the WAXS peaks.
[b] The intercalated clay was clay with an interlayer d-spacing greater than 1.9 nm.

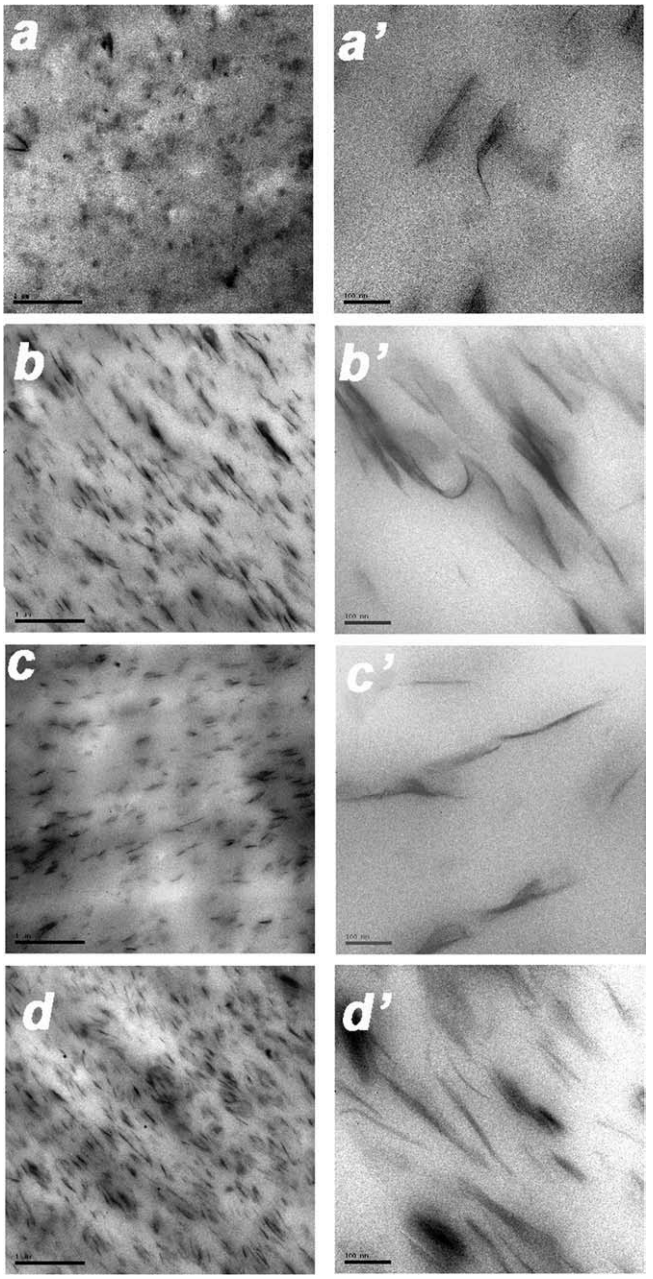

Figure 4 TEM micrographs of the NBR/OC15A clay nanocomposites as a function of the amount of clay and the dispersion procedure: (a) 2.5% clay (melt intercalation), (b) 5.0% clay (melt intercalation), (c) 2.5% clay (solution intercalation), and (d) 5.0% clay (solution intercalation). The micrographs on the right side were taken at a higher magnification.

Morphology

To confirm the different intercalation degrees of the layered organoclay structures, the morphology of the NBR-based nanocomposites was evaluated with TEM. Figure 4 shows TEM micrographs of vulcanized NBR/OC15A nanocomposites as a function of the clay-dispersion procedure.

In all samples, most of the clay particles (represented by dark regions) were stacked in the form of tactoids, and this confirmed that the NBR chains did not completely diffuse into all clay galleries, as also indicated by XRD results. However, these tactoids presented different thicknesses and sizes. Some were very thin (ca. 3–5 nm), and this indicated the presence of very few stacks in the tactoids. This morphology indicated a good dispersion of the clay platelets inside the NBR matrix. In addition, it is possible to observe in the higher magnification

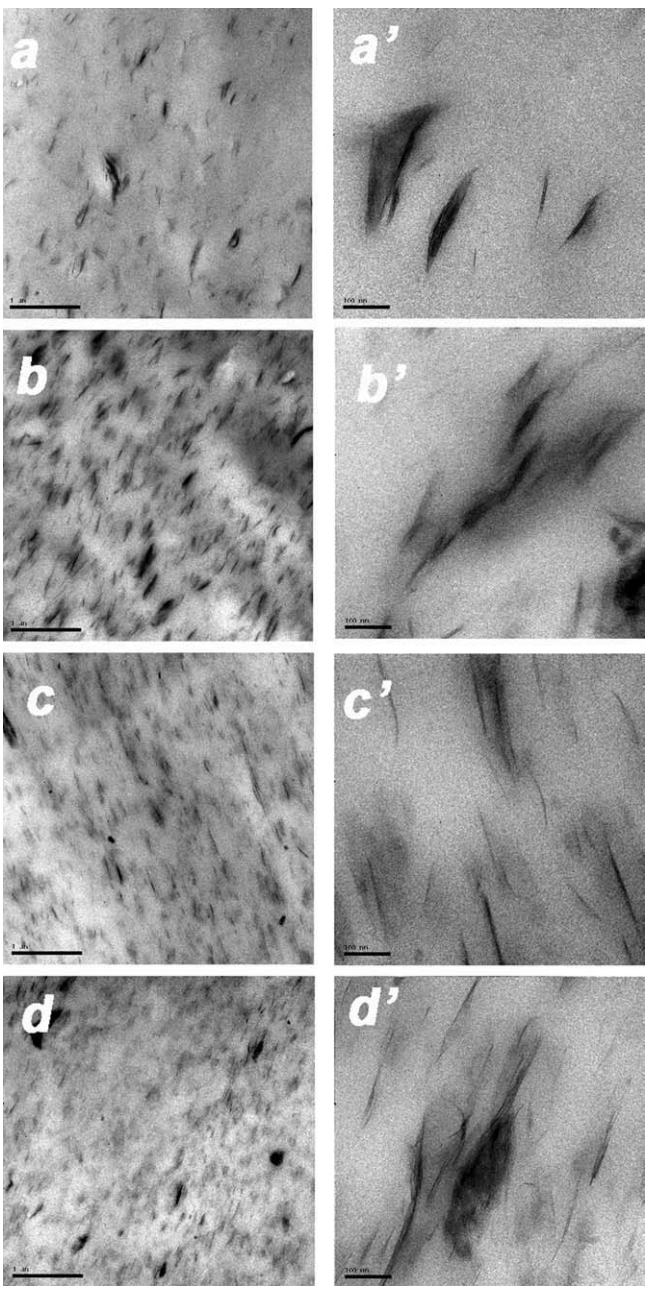

Figure 5 TEM micrographs of the NBR/OC30B clay nanocomposites as a function of the amount of clay and the dispersion procedure: (a) 2.5% clay (melt intercalation), (b) 5.0% clay (melt intercalation), (c) 2.5% clay (solution intercalation), and (d) 5.0% clay (solution intercalation). The micrographs on the right side were taken at a higher magnification.

micrographs a gap between the layers, which confirmed the intercalation of the polymer chains into some clay layers. The morphologies of the nanocomposites prepared by the solution-intercalation procedure [Fig. 4(d)] presented better clay dispersion and a lower number of aggregate structures. Despite the greater number of aggregates, some individual clay platelets (very few) could be observed.

The TEM micrographs of the NBR/OC30B nanocomposites are presented in Figure 5.

Despite the higher degree of intercalation indicated by the XRD experiments, these nanocomposites also presented a great number of aggregates (mainly those prepared by melt intercalation). The previous dispersion of the OC30B clay into the solvent resulted in thinner tactoids and also a small number of exfoliated silicate layers. In addition, there were fewer aggregates in some regions, which presented visible gaps between the layers; this indicated the intercalation process. The best degree of intercalation and the most uniform distribution of the clay inside the NBR matrix were reached with OC30B previously dispersed into the solvent. This result agreed with the XRD experiments and may have been due to the interaction between the OH groups of OC30B and the nitrile groups of the rubber.

Curing characteristics and physical properties

The curing characteristics of the nanocomposites were obtained at 170°C, and the data are summarized in Table III. The addition of 2.5% organoclay increased the minimum and maximum torque (M_L and M_H, respectively) and decreased t_{90} in comparison with the gum system. Among the filled systems, there was no significant influence of the amount of the filler on the curing parameters. The presence of OC30B resulted in slight increases in M_L and M_H versus the composites with similar proportions of OC15A, but the curing time was similar. Nanocomposites prepared by solution dispersion displayed higher M_H values, and the higher values were also observed for nanocomposites containing OC30B. The improvement of torque was an indication of improved filler–matrix interactions due to the good affinity between NBR and OC30B. All the nanocomposites presented a lower optimum curing time than the pure NBR, and this indicated that the organoclay accelerated the curing process. Similar behavior has been observed in rubber-based nanocomposites cured with sulfur systems.[11,35] Das et al.[24] also observed a small decrease in t_{90} for NBR-based nanocomposites cured with peroxide, but the difference between the gum and filled rubbers was not high. The accelerating action of the organoclay in our system was more effective, probably because of the presence of BMI as the curing coagent, which should have interacted with the quaternary ammonium salt present in the nanosilicate structure.

The physicomechanical properties of the NBR composites are also summarized in Table III as functions of the organoclay (the type of intercalant and amount) and the dispersion procedure of the clay. The presence of clay (as little as 2.5%) resulted in a significant improvement of the tensile strength and elongation at break, and this indicated an important reinforcing effect of these clays. The modulus increased with the addition of 5.0% clay (OC15A or OC30B), and this confirmed the reinforcing action of these fillers. For the nanocomposites prepared by melt intercalation, increasing the clay content resulted in a slight improvement in the tensile strength, regardless of the type of the intercalant in the organoclay. However, for the nanocomposites prepared by the solution procedure, the tensile

TABLE III
Curing Characteristics and Physicomechanical Properties of the NBR-Based Nanocomposites

Organoclay		Curing characteristics			Physicomechanical properties			
Type	Amount	M_H (N m)	M_L (N m)	t_{90} (min)	Ultimate tensile strength (MPa)	Elongation at break (%)	Modulus at 10% elongation (MPa)	Oil uptake (%)
—	0	2.6	0.38	10.5	2.5 ± 0.1	450 ±	2.7	0.5 ± 0.05
Melt-intercalation process								
OC15A	2.5	3.0	0.41	7.6	4.1 ± 0.5	730 ± 70	2.8	1.3 ± 0.12
OC15A	5.0	2.9	0.37	7.7	4.4 ± 0.1	720 ± 35	3.1	1.5 ± 0.13
OC30B	2.5	3.1	0.43	7.4	3.6 ± 0.2	640 ± 30	2.7	1.0 ± 0.10
OC30B	5.0	3.4	0.44	7.5	4.5 ± 0.2	670 ± 38	3.2	1.0 ± 0.08
Solution process								
OC15A	2.5	3.3	0.41	7.3	4.3 ±0.5	750 ± 67	3.0 ± 0.1	1.3 ± 0.11
OC15A	5.0	3.5	0.53	7.5	7.9 ± 1.2	630 ± 100	4.9 ± 0.7	1.9 ± 0.15
OC30B	2.5	3.4	0.51	7.3	6.3 ± 0.6	660 ± 45	3.5 ± 0.4	1.5 ± 0.10
OC30B	5.0	3.5	0.77	8.0	9.6 ± 1.0	270 ± 43	6.8 ± 0.8	1.4 ± 0.13

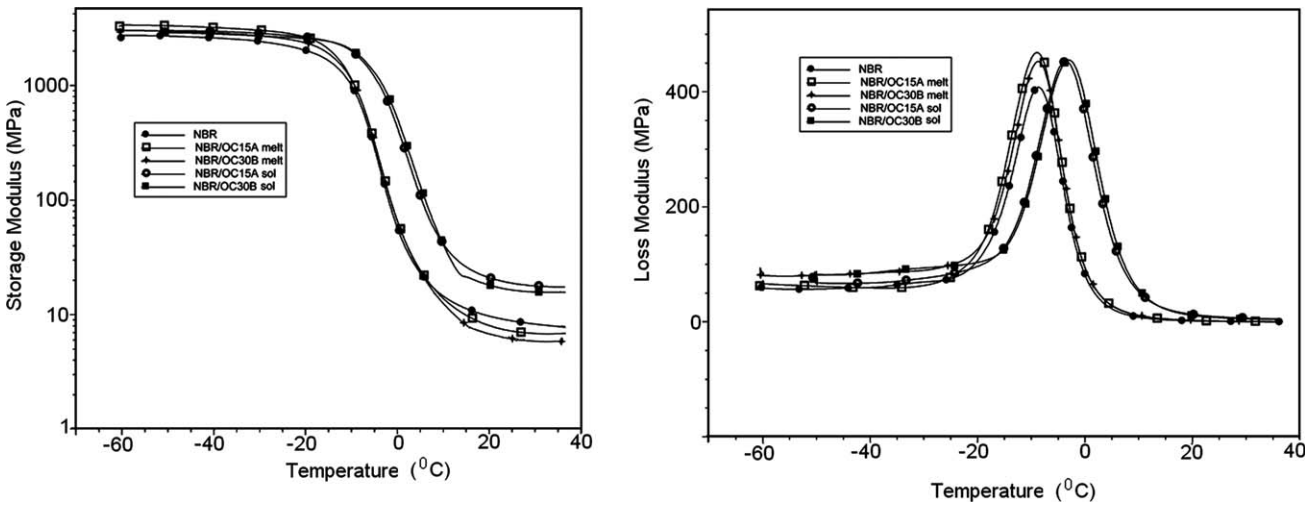

Figure 6 Dynamic mechanical properties of NBR-based nanocomposites with 5% organoclay as a function of the clay-dispersion procedure: (●) pure NBR, NBR/OC15A nanocomposites prepared by (□) melt and (○) solution dispersion, and NBR/OC30B nanocomposites prepared by (★) melt and (■) solution dispersion.

strength and modulus increased significantly with the amount of clay increasing in the composite. In addition, the composite containing OC30B had a higher tensile strength but a lower elongation at break. These results agreed with the XRD results, which indicated a higher exfoliation/intercalation degree of the clay in those nanocomposites prepared with the OC30B organoclay, and they confirmed that the good dispersion of the filler and good interactions between the filler and matrix are of paramount importance for better mechanical performance in nanocomposites.

The oil-uptake values increased with the addition of the organoclay, and this behavior was more accentuated for nanocomposites containing OC15A. This phenomenon indicated that the oil resistance decreased with the presence of the organoclay, probably because of the presence of the long aliphatic hydrocarbon chain in the organophilic clay, which had a good affinity for mineral oil. In this sense, nanocomposites prepared with OC15A, which had a greater number of hydrocarbon chains in the intercalant, also presented higher oil-uptake values.

DMA

The dynamic mechanical properties of the filled NBR composites were evaluated from −60 to +40°C. Figure 6 compares the dynamic mechanical properties of the melt- and solution-intercalated NBR-based nanocomposites containing 5% clay. The incorporation of OC15A or OC30B resulted in a slight increase in the storage modulus below T_g. Above T_g, the nanocomposites prepared by solution intercalation had higher values than the pure gum, and this confirmed the reinforcing effect when the clay was better dispersed in an intercalated and/or exfoliated form inside the rubber matrix. The storage moduli of the nanocomposites prepared by melt intercalation were slightly lower than those of the pure gum. Similar behavior was observed for nanocomposites containing 2.5% clay (not shown here).

The dependence of the loss modulus on the temperature is also presented Figure 6, and its maximum is considered T_g; the values are summarized in Table IV. All nanocomposites prepared with OC15A and OC30B displayed significant shifts of T_g toward higher values when the clay dispersion was performed in solution. These results suggested a decrease in the NBR chain mobility, probably as a result of a better intercalation degree of the polymer chains inside the clay galleries, and they confirmed that the solution-intercalation procedure resulted in higher filler dispersions and higher filler–matrix interactions. These results were in agreement with the microscopic behavior observed in XRD and TEM experiments.

Creep behavior

Figure 7 illustrates the creep compliance behavior and strain recovery of the gum NBR and the filled nanocomposites. Table IV also summarizes the creep parameters. The shape of the creep curves of the composites was very similar to that of the pure NBR gum, but their creep compliance values were significantly smaller; this confirmed the reinforcing effect of theses layered silicates in the NBR matrix. Similar improvements have been reported by other authors.[29–30,36]

The lowest creep compliance values were found in nanocomposites prepared with OC30B [5% clay dispersed by the solution process, Fig. 7(k), or 2.5% clay dispersed by the melt process, Fig. 7(d)]. These

TABLE IV
Dynamical Mechanical Data for the NBR-Based Nanocomposites

	Organoclay			Dynamic mechanical parameters as a function of the temperature			
NBR	Type	Amount	Creep recovery (%)	Storage modulus at −40°C (MPa)	Storage modulus at 40°C (MPa)	Tan δ	T_g (°C)
100	—	0	97	2640	8	1.4	−8.9
Melt-intercalation process							
97.5	OC15A	2.5	88	3490	7.4	1.4	−8.0
95.0	OC15A	5.0	92	3230	6.8	1.4	−9.0
97.5	OC30B	2.5	97	2540	3.5	1.6	−7.5
95.0	OC30B	5.0	94	2870	4.0	1.4	−8.9
Solution process							
97.5	OC15A	2.5	91	2560	8	1.4	−7.4
95.0	OC15A	5.0	96	3430	12.4	1.4	−3.7
97.5	OC30B	2.5	97	3280	24.5	1.3	−1.8
95.0	OC30B	5.0	97	2830	15.7	1.4	−3.2

samples also presented the highest creep recovery (see Table IV). Nanocomposites containing OC15A presented a good creep compliance response (low deformation under static force) when 5% clay was dispersed by the solution procedure [Fig. 7(g)]. The creep compliance values reflected the dispersion state of the layered silicate. A higher dispersion state resulted in lower creep compliance, that is, higher resistance to deformation under a constant stress. OC30B was able to disperse inside NBR to a higher extent because of the better interaction between the filler and matrix. In this sense, with the melt procedure, it was necessary to employ only 2.5% OC30B to achieve almost the same performance as that reached with the solution-intercalation procedure. A higher amount of OC30B clay with melt intercalation [Fig. 7(e)] was not a good choice for good creep performance, probably because of the higher number of aggregates, which decreased the extent of filler–matrix interactions. This result was very important because it was possible to avoid the ecological problem of working with the solvent. After discontinuation of the creep load, the best strain recovery values were achieved with pure NBR, with the nanocomposites containing OC30B prepared in solution or melt, and with the nanocomposites containing 5% OC15A prepared in solution. As observed in TEM micrographs, a higher amount of OC30B resulted in a higher amount of aggregated clay, which reduced the extent of filler–matrix interactions.

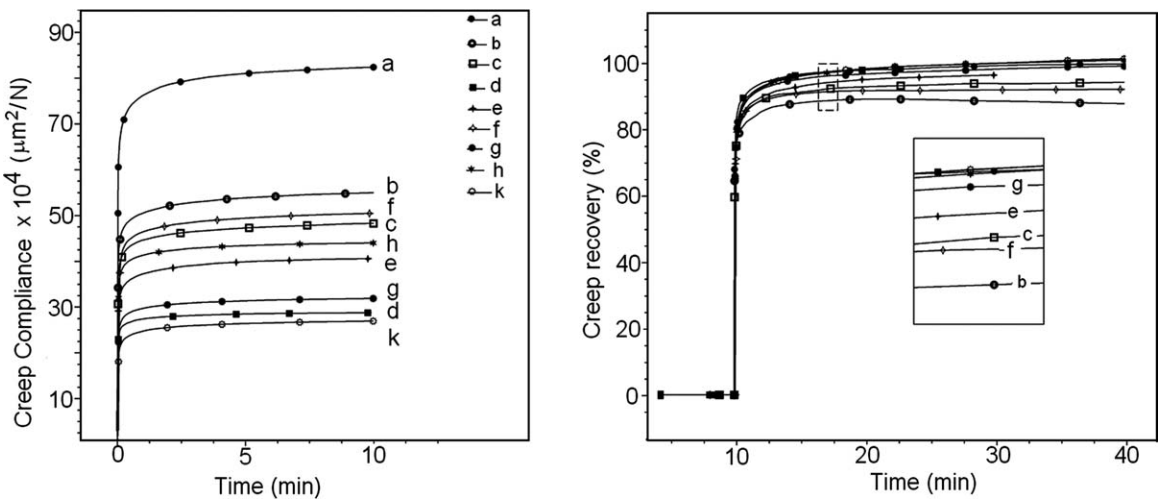

Figure 7 Creep compliance behavior and strain recovery of NBR and filled nanocomposites: (a) pure NBR, (b) 2.5% OC15A clay (melt intercalation), (c) 5.0% OC15A clay (melt intercalation), (d) 2.5% OC30B clay (melt intercalation), (e) 5.0% OC30B clay (melt intercalation), (f) 2.5% OC15A clay (solution intercalation), (g) 5.0% OC15A clay (solution intercalation), (h) 2.5% OC30B clay (solution intercalation), and (k) 5.0% OC30B clay (solution intercalation).

CONCLUSIONS

This article reports the efficiency of two different organoclays with respect to the degree of exfoliation/intercalation in NBR-based nanocomposites and the effect of the extent of the dispersion on the physicomechanical properties of the corresponding rubber-based nanocomposites. On the basis of the results obtained in this report, it is possible to suggest that the best intercalation of NBR chains into a layered clay, in both melt and solution processes, was achieved with OC30B, an organoclay that contains polar groups in the intercalant and improves interactions with polar rubbers such as NBR. This behavior was demonstrated by wide-angle X-ray scattering (WAXS) and TEM. The solution process was more effective for the intercalation process than melt intercalation. In all cases, an improvement in the tensile properties, such as the ultimate tensile strength and modulus, was observed, and this indicated a good reinforcing action of the clays. Also, the best tensile strength was achieved with the solution-intercalation process, and this suggests that the good dispersion of the clay is a very important factor for the improvement of the mechanical properties. As for the solution process, the nanocomposites prepared with OC30B displayed higher tensile strength.

The creep results were very sensitive to the dispersion degree of the layered clay inside NBR. A significant reduction of the creep compliance values and high strain recovery after creep experiments were observed for the systems filled with OC30B. These results confirm that better physicomechanical performance and creep behavior are achieved in systems containing clay with a higher degree of exfoliation/intercalation, and this feature in NBR-based systems is achieved when the clay is previously dispersed in a solution of NBR.

References

1. Goettler, L. A.; Lee, K. Y.; Thakkar, H. Polym Rev 2007, 47, 291.
2. Pavlidou, S.; Papaspyrides, C. D. Prog Polym Sci 2008, 33, 1119.
3. Karger-Kocsis, J.; Wu, C. M. Polym Eng Sci 2004, 44, 1083.
4. Varghese, S. S.; Karger-Kocsis, J. J Appl Polym Sci 2004, 91, 813.
5. Wu, Y.-P.; Jia, Q. X.; Yu, D. S.; Zhang, L. Q. J Appl Polym Sci 2003, 89, 3855.
6. Hwang, W. G.; Wei, K. H.; Wu, C. M. Polymer 2004, 45, 5729.
7. Kader, M. A.; Kim, K.; Lee, Y. S.; Nah, C. J Mater Sci 2006, 41, 7341.
8. Sadhu, S.; Bhowmick, A. K. J Polym Sci Part B: Polym Phys 2004, 42, 1573.
9. Sadhu, S.; Bhowmick, A. K. J Polym Sci Part B: Polym Phys 2005, 43, 1854.
10. Sadhu, S.; Bhowmick, A. K. Rubber Chem Technol 2005, 78, 321.
11. Choi, D.; Kader, M. A.; Cho, B. H.; Huh, Y.; Nah, C. J Appl Polym Sci 2005, 98, 1688.
12. Kim, J. T.; Oh, T. S.; Lee, D. H. Polym Int 2003, 52, 1058.
13. Kim, J. T.; Oh, T. S.; Lee, D. H. Polym Int 2004, 53, 406.
14. Kim, J. T.; Lee, D. Y.; Oh, T. S.; Lee, D. H. J Appl Polym Sci 2003, 89, 2633.
15. Kim, J. T.; Oh, T. S.; Lee, D. H. Polym Int 2003, 52, 1203.
16. Liu, L.; Jia, D.; Luo, Y.; Guo, B. J Appl Polym Sci 2006, 100, 1905.
17. Kim, Y.; White, J. L. J Appl Polym Sci 2005, 96, 1888.
18. Nah, C.; Ryu, H. J.; Kim, W. D.; Chang, Y.-W. Polym Int 2003, 52, 1359.
19. Kim, S. H.; Chung, J. W.; Kang, T. J.; Kwak, S. Y.; Suzuki, T. Polymer 2007, 48, 4271.
20. Liang, Y.-R.; Cao, W.-L.; Zhang, X.-B.; Tan, Y.-J.; He, S.-J.; Zhang, L.-Q. J Appl Polym Sci 2009, 112, 3087.
21. Nah, C.; Ryu, H. J.; Kim, W. D.; Choi, S.-S. Polym Adv Technol 2002, 13, 649.
22. Nah, C.; Ryu, H. J.; Han, S. H.; Rhee, J. M.; Lee, M.-H. Polym Int 2001, 50, 1265.
23. Han, M.; Kim, H.; Kim, E. Nanotechnology 2006, 17, 403.
24. Das, A.; Jurk, R.; Stöckelhuber, W.; Heinrich, G. Macromol Mater Eng 2008, 293, 479.
25. Das, A.; Jurk, R.; Stöckelhuber, W.; Heinrich, G. Express Polym Lett 2007, 1, 717.
26. Fritzsche, J.; Das, A.; Jurk, R.; Stöckelhuber, W.; Heinrich, G.; Klüppel, M. Express Polym Lett 2008, 2, 373.
27. González, L.; Rodriguez, A.; Marcos, A.; Chamorro, C. Rubber Chem Technol 1996, 69, 203.
28. Inoue, T. J Appl Polym Sci 1994, 54, 709.
29. Siengchin, S.; Karger-Kocsis, J. Macromol Rapid Commun 2006, 27, 2090.
30. Siengchin, S.; Karger-Kocsis, J.; Thomann, R. Express Polym Lett 2008, 2, 746.
31. Tiwari, R. R.; Khilar, K. C.; Natarajan, U. Appl Clay Sci 2008, 38, 203.
32. Lu, Y.-L.; Liang, Y.-R.; Wu, Y.-P.; Zhang, L.-Q. Macromol Mater Eng 2006, 291, 27.
33. Liang, Y.-R.; Ma, J.; Lu, Y.-L.; Wu, Y.-P.; Zhang, L.-Q.; Mai, Y.-W. J Polym Sci Part B: Polym Phys 2005, 43, 2653.
34. Gatos, K. G.; Szazdi, L.; Pukanszky, B.; Karger-Kocsis, J. Macromol Rapid Commun 2005, 26, 915.
35. Mousa, A.; Karger-Kocsis, J. Macromol Mater Eng 2001, 286, 260.
36. Lietz, S.; Yang, J.-L.; Bosch, E.; Sandler, J. K. W.; Zhang, Z.; Altstädt, V. Macromol Mater Eng 2007, 292, 23.